J|A|C|S ARTICLES

Published on Web 06/15/2009

Anisotropic Magnetic Behavior of Anionic Ce@C_{82} Carbene Adducts

Yuta Takano,[†] Motoki Aoyagi,[†] Michio Yamada,[†] Hidefumi Nikawa,[†] Zdenek Slanina,[†] Naomi Mizorogi,[†] Midori O. Ishitsuka,[†] Takahiro Tsuchiya,[†] Yutaka Maeda,[‡] Takeshi Akasaka,*[,†] Tatsuhisa Kato,[§] and Shigeru Nagase*[,||]

Center for Tsukuba Advanced Research Alliance, University of Tsukuba, Tsukuba, Ibaraki 305-8577, Japan, Department of Chemistry, Tokyo Gakugei University, Koganei, Tokyo 184-8501, Japan, Department of Chemistry, Josai University, Sakaido, Saitama 350-0295, Japan, and Department of Theoretical and Computational Molecular Science, Institute for Molecular Science, Okazaki, Aichi 444-8585, Japan

Received March 18, 2009; E-mail: akasaka@tara.tsukuba.ac.jp; nagase@ims.ac.jp

Abstract: Derivatives of Ce@C_{82}(C_{2v}) have been synthesized and fully characterized, and their anisotropic magnetism has been observed as paramagnetic shifts in NMR measurements. Carbene addition by photochemical reaction afforded two isomers of Ce@C_{82}(C_{2v})Ad (Ad = adamantylidene), **2a** and **2b**, demonstrating high regioselectivity. The two isomers were characterized using MALDI−TOF mass spectrometry, vis−NIR absorption spectroscopy, ^{1}H and ^{13}C NMR spectroscopy, and electrochemistry. The structure of the minor isomer (**2b**) was elucidated by single-crystal X-ray structural analysis. ^{13}C and ^{1}H NMR measurements revealed the characteristic anisotropic interaction between the f electron on the Ce atom and nuclear spins of the carbon atoms of the cage and the protons of the Ad group, respectively.

Introduction

Endohedral metallofullerenes (EMFs) have attracted special interest as new spherical molecules because they have unusual physical and chemical properties that are imparted by the encapsulated metal atoms.[1−3] As a novel hybrid material of metals and fullerenes, EMFs are expected to have a wide range of potential applications in chemistry, physics, biomedicine, and nanomaterials science.[4,5]

From a magnetism aspect, rare-earth-encapsulating EMFs, such as La@C_{82},[6−8] Ce@C_{82},[7,9−11] Gd@C_{82},[6,12−16] and so on,[13−17] are of particular interest because the interplay between the spins of the metal atoms and the π-electron spins of the cage is expected to produce unconventional magnetic features. Among many kinds of EMFs, Ce@C_{82}(C_{2v}) is considered as a simple free-spin model of EMFs because the Ce atom inside the cage has a 4f^{1} electronic structure.[18,19] [Hereafter,

[†] University of Tsukuba.
[‡] Tokyo Gakugei University.
[§] Josai University.
[||] Institute for Molecular Science.

(1) For a review, see: Bethune, D. S.; Johnson, R. D.; Salem, J. R.; Devries, M. S.; Yannoni, C. S. *Nature* **1993**, *366*, 123.
(2) For a review, see: *The Chemistry of Fullerenes*; Taylor, R., Ed.; World Scientific Publishing: Singapore, 1995.
(3) For a review, see: Akasaka, T., Nagase, S., *Endofullerenes: A New Family of Carbon Clusters*; Kluwer Academic Publishers: Dordrecht, The Netherlands, 2002.
(4) (a) Thrash, T. P.; Cagle, D. W.; Alford, J. M.; Wright, K.; Ehrhardt, G. J.; Mirzadeh, S.; Wilson, L. J. *Chem. Phys. Lett.* **1999**, *308*, 329. (b) Mikawa, M.; Kato, H.; Okumura, M.; Narazaki, M.; Kanazawa, Y.; Miwa, N.; Shinohara, H. *Bioconjugate Chem.* **2001**, *12*, 510. (c) Kato, H.; Kanazawa, Y.; Okumura, M.; Taninaka, A.; Yokokawa, T.; Shinohara, H. *Acad. Radiol.* **2002**, *9*, S495. (d) Bolskar, R. D.; Benedetto, A. F.; Husebo, L. O.; Price, R. E.; Jackson, E. F.; Wallace, S.; Wilson, L. J.; Alford, J. M. *J. Am. Chem. Soc.* **2003**, *125*, 5471. (e) Okumura, M.; Mikawa, M.; Yokokawa, T.; Kanazawa, Y.; Kato, H.; Shinohara, H. *J. Am. Chem. Soc.* **2003**, *125*, 4391. (f) Sitharaman, B.; Bolskar, R. D.; Rusakova, I.; Wilson, L. J. *Nano Lett.* **2004**, *4*, 2373. (g) Tóth, E.; Bolskar, R. D.; Borel, A.; González, G.; Helm, L.; Merbach, A. E.; Shitaraman, B.; Wilson, L. J. *J. Am. Chem. Soc.* **2005**, *127*, 799. (h) Yanagi, K.; Okubo, S.; Okazaki, T.; Kataura, H. *Chem. Phys. Lett.* **2007**, *435*, 306. (i) Zhang, E. Y.; Shu, C. Y.; Feng, L.; Wang, C. R. *J. Phys. Chem. B* **2007**, *111*, 14223.
(5) (a) Huang, H. J.; Yang, S. H. *J. Organomet. Chem.* **2000**, *599*, 42. (b) Yang, S. F.; Yang, S. H. *J. Phys. Chem. B* **2001**, *105*, 9406. (c) Nakashima, N.; Sakai, M.; Murakami, H.; Sagara, T.; Wakahara, T.; Akasaka, T. *J. Phys. Chem. B* **2002**, *106*, 3523. (d) Li, X. G.; Yang, S. F.; Yang, S. H.; Xu, Y.; Liu, Y. Q.; Zhu, D. B. *Thin Solid Films* **2002**, *413*, 231. (e) Yang, S. F.; Fan, L. Z.; Yang, S. H. *J. Phys. Chem. B* **2003**, *107*, 8403. (f) Yang, S.; Fan, L.; Yang, S. *J. Phys. Chem. B* **2004**, *108*, 4394. (g) Yasutake, Y.; Shi, Z.; Okazaki, T.; Shinohara, H.; Majima, Y. *Nano Lett.* **2005**, *5*, 1057. (h) Yumura, T.; Sato, Y.; Suenaga, K.; Urita, K.; Iijima, S. *Nano Lett.* **2006**, *6*, 1389. (i) Tsuchiya, T.; Sato, K.; Kurihara, H.; Wakahara, T.; Maeda, Y.; Akasaka, T.; Ohkubo, K.; Fukuzumi, S.; Kato, T.; Nagase, S. *J. Am. Chem. Soc.* **2006**, *128*, 14418. (j) Tang, J.; Xing, G.; Zhao, Y.; Jing, L.; Yuan, H.; Zhao, F.; Gao, X.; Qian, H.; Su, R.; Ibrahim, K.; Chu, W.; Zhang, L.; Tanigaki, K. *J. Phys. Chem. B* **2007**, *111*, 11929. (k) Perez-Jimenez, A. J. *J. Phys. Chem. C* **2007**, *111*, 17640. (l) Tsuchiya, T.; et al. *J. Am. Chem. Soc.* **2008**, *130*, 450.
(6) Funasaka, H.; Metals, K. S.; Yamamoto, K.; Takahashi, T. *J. Phys. Chem.* **1995**, *99*, 1826.
(7) Nuttall, C. J.; Inada, Y.; Nagai, K.; Iwasa, Y. *Phys. Rev. B* **2000**, *62*, 8592.
(8) Iwasa, Y.; Nuttall, C. J. *Synth. Met.* **2003**, *135*, 773.
(9) Nuttall, C. J.; Watanabe, Y.; Inada, Y.; Nagai, K.; Muro, T.; Chi, D. H.; Takenobu, T.; Iwasa, Y.; Kikuchi, K. In *Electronic Properties of Novel Materials: Science and Technology of Molecular Nanostructures*; Kuzmany, H., Fink, J., Mehring, M., Roth, S., Eds.; American Institute of Physics: New York, 1999; Vol. 486, p 115.
(10) Nuttall, C. J.; Inada, Y.; Watanabe, Y.; Nagai, K.; Muro, T.; Chi, D. H.; Takenobu, T.; Iwasa, Y.; Kikuchi, K. *Mol. Cryst. Liq. Cryst. Sci. Technol., Sect. A* **2000**, *340*, 635.
(11) Inakuma, M.; Kato, H.; Taninaka, A.; Shinohara, H.; Enoki, T. *J. Phys. Chem. B* **2003**, *107*, 6965.

 10.1021/ja902106a CCC: $40.75

Ce@$C_{82}(C_{2v})$ and La@$C_{82}(C_{2v})$ will be denoted simply as Ce@C_{82} and La@C_{82}, respectively]. Recently, we reported the temperature dependence of ^{13}C NMR measurements of Ce@C_{82} in solution, which originates from the spin−spin interaction between the nuclear spins of carbon atoms of the cage and the f electron spin remaining on the Ce atom.[18i,20] Inakuma and co-workers reported the magnetic anisotropy of Ce@C_{82} by examining the field-induced change in the magnetic susceptibility of organic solutions of Ce@C_{82} and the temperature dependence of the magnetic susceptibility and magnetization of Ce@C_{82} solid films.[11] To date, however, no article has reported the spin−spin interactions and anisotropic magnetism of chemically functionalized EMFs having paramagnetic carbon cage structures. Furthermore, there have been only a few studies of chemical modifications of Ce@C_{82},[18j,21,22] and to the best of our knowledge, none of the reports achieved structural elucidations of the derivatives. In view of the promising potential applications of EMFs in the nanotechnology area, it is very interesting and important to clarify the influence of chemical modifications of EMFs on their magnetic properties.

Carbene addition is an efficient method for preparing derivatives of M@C_{82} (M = La, Ce and Gd). We recently reported the reaction of adamantylidene (Ad) with La@C_{82}, which affords only two isomers in high yield (up to 80%).[23] The structure of the major isomer, La@C_{82}Ad-I (**3a**), was unambiguously determined by X-ray crystallographic characterization.[23a] However, the structure of the minor isomer, La@C_{82}Ad-II (**3b**), has not been definitively elucidated.[23b]

Here we present the first isolation and full characterization of the analogous derivatives of Ce@C_{82}, namely, Ce@C_{82}Ad-I (**2a**) and Ce@C_{82}Ad-II (**2b**), including single-crystal X-ray structural analysis for the minor isomer **2b**. The anisotropic interactions between the f-electron spin of the Ce atom and the nuclear spins of the carbon cage and the addend in **2a** and **2b** in their anionic forms, which were observed via temperature-dependent ^{1}H and ^{13}C NMR chemical shifts, are also discussed.

Experimental Section

General. All of the chemicals and solvents were obtained from Wako and Aldrich and used without further purification, unless otherwise stated. Toluene was distilled over benzophenone sodium ketyl under an argon atmosphere prior to use in reaction. 1,2-Dichlorobenzene (ODCB) was distilled over P_2O_5 under vacuum prior to use. High-performance liquid chromatography (HPLC) isolation was performed on an LC-908 chromatograph (Japan Analytical Industry Co., Ltd.) monitored by UV absorption at 330 nm. Toluene was used as the eluent. Mass spectrometry was performed on a Bruker BIFLEX III instrument with 1,1,4,4-tetraphenyl-1,3-butadiene as the matrix. Absorption spectra were measured by using a SHIMADZU UV-3150 spectrophotometer. The ^{1}H and ^{13}C NMR measurements were carried out on a Bruker AVANCE 500 with a CryoProbe system. Tetramethylsilane was used as an internal reference ($\delta = 0.00$ ppm). J_{HH} coupling constants could not be determined because of the paramagnetic shift. Signals of the carbon atoms on the Ad group were not detected because they were obscured by the signals of the electrolyte and acetone. Cyclic voltammograms (CVs) and differential pulse voltammograms (DPVs) were recorded on a BAS CV50W electrochemical analyzer. Platinum wires were used as the working and counter electrodes. The reference electrode was a saturated calomel reference electrode (SCE) filled with 0.1 M (n-Bu)$_4$NPF$_6$ (TBAPF$_6$) in ODCB. CVs were recorded using a scan rate of 20 mV/s, and DPVs were obtained using a pulse amplitude of 50 mV, a pulse width of 50 ms. a pulse period of 200 ms, and a scan rate of 20 mV/s.

An ordinary Ce@C_{82} sample was prepared according to a procedure reported elsewhere.[24] An 11% ^{13}C-enriched Ce@C_{82} sample was prepared by a similar procedure using a composite anode of ^{13}C-enriched graphite and cerium oxide instead of an ordinary graphite and cerium oxide rod.

Synthesis of Adamantyl Derivatives of Ce@C_{82}. AdN_2 (**1**) was synthesized and purified as reported in the literature.[25] An excess amount of **1** (6.2 mg, 3.8×10^{-4} mol) was added to a 8.0×10^{-5} M toluene solution of Ce@C_{82} (5.6 mg, 5.0×10^{-6} mol), and the mixture was degassed by freeze−pump−thaw cycles and then irradiated using a high-pressure mercury-arc lamp (cutoff <350 nm) for 90 s. The two isomers **2a** and **2b**, were isolated from the

(12) Funasaka, H.; Sakurai, K.; Oda, Y.; Yamamoto, K.; Takahashi, T. *Chem. Phys. Lett.* **1995**, *232*, 273.
(13) Huang, H. J.; Yang, S. H.; Zhang, X. X. *J. Phys. Chem. B* **1999**, *103*, 5928.
(14) Huang, H. J.; Yang, S. H.; Zhang, X. X. *J. Phys. Chem. B* **2000**, *104*, 1473.
(15) Kitaura, R.; Okimoto, H.; Shinohara, H.; Nakamura, T.; Osawa, H. *Phys. Rev. B* **2007**, *76*, 172409.
(16) Nadai, C. D.; Mirone, A.; Dhesi, S. S.; Bencok, P.; Brookes, N. B.; Marenne, I.; Rudolf, P.; Tagmatarchis, N.; Shinohara, H.; Dennis, T. J. S. *Phys. Rev. B* **2004**, *69*, 184421.
(17) Bondino, F.; Cepek, C.; Tagmatarchis, N.; Prato, M.; Shinohara, H.; Goldoni, A. *J. Phys. Chem. B* **2006**, *110*, 7289.
(18) (a) Suzuki, S.; Torisu, H.; Kubota, H.; Wakabayashi, T.; Shiromaru, H.; Achiba, Y. *Int. J. Mass. Spectrom. Ion Processes* **1994**, *138*, 297. (b) Ding, J.; Weng, L.-T.; Yang, S. *J. Phys. Chem.* **1996**, *100*, 11120. (c) Suzuki, T.; Kikuchi, K.; Oguri, F.; Nakao, Y.; Suzuki, S.; Achiba, Y.; Yamamoto, K.; Funasaka, H.; Takahashi, T. *Tetrahedron* **1996**, *52*, 4973. (d) Liu, B. B.; Zou, G. T.; Yang, H. B.; Yu, S.; Lu, J. S.; Liu, Z. Y.; Liu, S. Y.; Xu, W.-G. *J. Phys. Chem. Solids* **1997**, *58*, 1873. (e) Lebedkin, S.; Renker, B.; Heid, R.; Schober, H.; Rietschel, H. *Appl. Phys. A: Mater. Sci. Process.* **1998**, *66*, 273. (f) Nuttall, C. J.; Inada, Y.; Watanabe, Y.; Nagai, K.; Muro, T.; Chi, D. H.; Takenobu, T.; Iwasa, Y.; Koichi, K. *Mol. Cryst. Liq. Cryst.* **2000**, *340*, 635. (g) Kodama, T.; Kusuda, M.; Ozawa, N.; Fujii, R.; Sakaguchi, K.; Nishikawa, H.; Ikemoto, I.; Kikuchi, K.; Miyake, Y.; Achiba, Y. *New Diamond Front. Carbon Technol.* **2001**, *11*, 367. (h) Shibata, K.; Rikiishi, Y.; Hosokawa, T.; Haruyama, Y.; Kubozono, Y.; Kashino, S.; Uruga, T.; Fujiwara, A.; Kitagawa, H.; Takano, T.; Iwasa, Y. *Phys. Rev. B* **2003**, *68*, 094104. (i) Solodovnikova, S. P.; Lebedkin, S. F. *Russ. Chem. Bull., Int. Ed.* **2003**, *52*, 1111. (j) Wakahara, T.; Kobayashi, J.; Yamada, M.; Maeda, Y.; Tsuchiya, T.; Okamura, M.; Akasaka, T.; Waelchli, M.; Kobayashi, K.; Nagase, S.; Kato, T.; Kako, M.; Yamamoto, K.; Kadish, K. M. *J. Am. Chem. Soc.* **2004**, *126*, 4883. (k) Woolley, R. A. J.; Schulte, K. H. G.; Wang, L.; Moriarty, P. J.; Cowie, B. C. C.; Shinohara, H.; Kanai, M.; Dennis, T. J. S. *Nano Lett.* **2004**, *4*, 361. (l) Rikiishi, Y.; Kubozono, Y.; Hosokawa, T.; Shibata, K.; Haruyama, Y.; Takabayashi, Y.; Fujiwara, A.; Kobayashi, S.; Mori, S.; Iwasa, Y. *J. Phys. Chem. B* **2004**, *108*, 7580. (m) Wang, L.; Schulte, K.; Woolley, R. A. J.; Kanai, M.; Dennis, T. J. S.; Purton, J.; Patel, S.; Gorovikov, S.; Dhanak, V. R.; Smith, E. F.; Cowie, B. C. C.; Moriarty, P. *Surf. Sci.* **2004**, *564*, 156. (n) Schulte, K.; Wang, L; Moriarty, P. J.; Purton, J.; Patel, S.; Shinohara, H.; Kanai, M.; Dennis, T. J. S. *Phys. Rev. B* **2005**, *71*, 115437.
(19) (a) Nagase, S.; Kobayashi, K. *Chem. Phys. Lett.* **1994**, *228*, 106. (b) Kemner, E.; Zerbetto, F.; Andreoni, W.; Curioni, A. *Phys. Rev. Lett.* **1996**, *77*, 834. (c) Muthukumar, K.; Larsson, J. A. *J. Phys. Chem. A* **2008**, *112*, 1071.
(20) Yamada, M.; Wakahara, T.; Lian, Y.; Tsuchiya, T.; Akasaka, T.; Waelchli, M.; Mizorogi, N.; Nagase, S.; Kadish, K. M. *J. Am. Chem. Soc.* **2006**, *128*, 1400.
(21) Hao, C.; Liu, Z.; Guo, X.; Liu, Z.; Xu, W.; Sun, Y.; Liu, S. *Rapid Commun. Mass. Spectrom.* **1997**, *11*, 1677.
(22) Maeda, Y.; Miyashita, J.; Hasegawa, T.; Wakahara, T.; Tsuchiya, T.; Feng, L.; Lian, Y.; Akasaka, T.; Kobayashi, K.; Nagase, S.; Kako, M.; Yamamoto, K.; Kadish, K. M. *J. Am. Chem. Soc.* **2005**, *127*, 2143.
(23) (a) Maeda, Y.; et al. *J. Am. Chem. Soc.* **2004**, *126*, 6858. (b) Matsunaga, Y.; Maeda, Y.; Wakahara, T.; Tsuchiya, T.; Ishitsuka, M. O.; Akasaka, T.; Mizorogi, N.; Kobayashi, K.; Nagase, S.; Kadish, K. M. *ITE Lett.* **2006**, *7*, C1.
(24) Yamamoto, K.; Funasaka, T.; Takahashi, T.; Akasaka, T.; Suzuki, T.; Maruyama, Y. *J. Phys. Chem.* **1994**, *98*, 12831.
(25) *Chemistry of Diazirines*; Liu, M. T. H., Ed.; CRC Press: Boca Raton, FL, 1987; Vols. 1 and 2.

Scheme 1

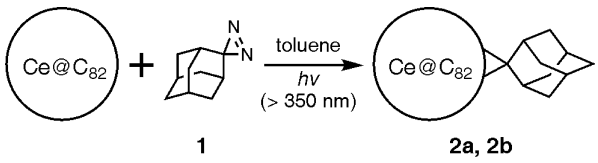

unreacted starting materials and multiadducts by one-step HPLC separation. Spectral data for **2a** and **2b** are given in the Supporting Information.

Preparation of the Anions of 2a and 2b. To prepare anions, the following procedures were done for **2a** and **2b**. Controlled-potential bulk electrolysis was performed using an H-type cell with two platinum gauze electrodes as the working and counter electrodes. $[Ce@C_{82}Ad]^-$ was obtained under argon in ODCB containing 0.2 M $TBAClO_4$ by setting the applied potential at a value 250 mV more negative than the $E_{1/2}$ value of the $[Ce@C_{82}Ad]^-/Ce@C_{82}Ad$ redox couple. The freshly prepared $[Ce@C_{82}Ad]^-$ was then transferred from the bulk cell to a 1.00 cm quartz cuvette under argon for measurement of its vis−NIR spectrum. The excess supporting electrolyte was precipitated from the solvent by adding carbon disulfide to the ODCB and then removed by filtration. The solvent was evaporated under reduced pressure. The residual brown solid was washed with hexane, dried, and dissolved in 1:3 (v/v) acetone-d_6/CS_2 for NMR analysis.

Theoretical Calculations for $Ce@C_{82}$, 2a, and 2b. Geometries were optimized with the Gaussian 03 program[26] using density functional theory (DFT) at the B3LYP level.[27−29] The relativistic effective core potential and SDD[30] basis set were used for Ce. The split-valence 3-21G basis set was used for C and H[31] (this method is denoted as B3LYP/3-21G∼SDD).

Thermal Isomerization of 2a to 2b. Powdered **2a** (0.93 mg, 7.4×10^{-7} mol) was placed in a glass tube and sealed under vacuum. The tube was heated in an oil bath at 250 °C for 12 h, after which the black powder in the tube was dissolved in CS_2. The solvent was replaced with toluene, and this was followed by HPLC analysis, which demonstrated that the black powder contained 20% **2a** and 80% **2b** (Figure S4 in the Supporting Information).

Results and Discussion

Irradiation of a toluene solution of $Ce@C_{82}$ with an excess molar amount of **1** resulted in the formation of the corresponding adducts (**2a** and **2b** in Scheme 1). **2a** and **2b** were purified by single-stage HPLC in 63 and 23% yields based on consumption of the starting $Ce@C_{82}$, respectively (see Figure 1 and the Supporting Information). This result indicates the striking similarity in the reactivities of $Ce@C_{82}$ and $La@C_{82}$ toward carbene addition.[23]

Figure 2 shows the vis−NIR absorption spectra of **2a** and **2b**. The absorption features of **2a** and **2b** are almost identical to those of pristine $Ce@C_{82}$ in the NIR field. This suggests that **2a** and **2b** retain the essential electronic structural characteristics of $Ce@C_{82}$, indicating that the π conjugation of the C_{82} cage is changed only slightly despite the C−C bond cleavage due to the carbene addition. From the similarities between the spectra of **2a** and **3a** and **2b** and **3b** (inset of Figure 2), it is reasonable to consider the respective addition sites to be the same, because the similarities indicate that they have similar fingerprints of the π-electron system topology.

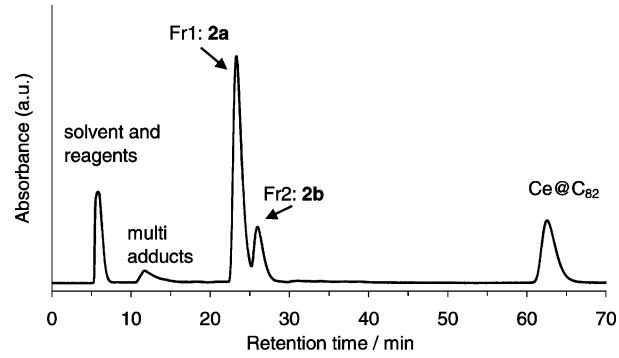

Figure 1. HPLC separation/isolation scheme for **2a** and **2b**. Conditions: Buckyprep column (ϕ20 mm × 250 mm); eluent, toluene; flow rate, 9.9 mL/min; wavelength, 330 nm; temperature, room temperature.

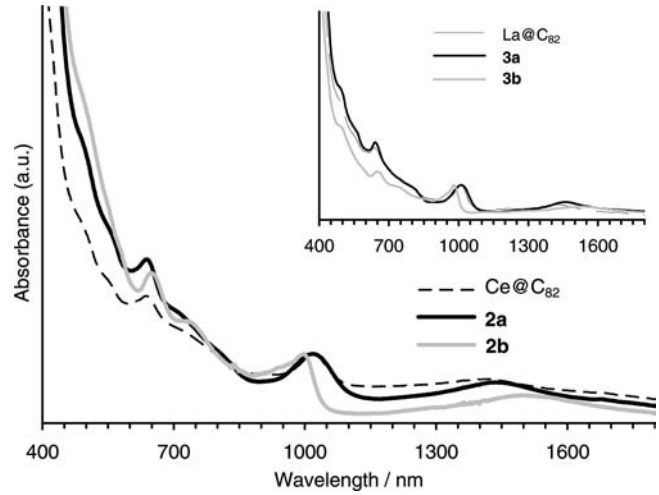

Figure 2. Vis−NIR absorption spectra of **2a**, **2b**, and $Ce@C_{82}$ in CS_2. Inset: spectra of **3a**, **3b**, and $La@C_{82}$ in CS_2 for comparison.

Table 1. Redox Potentials[a,b]

compound	$E^{(1)}_{ox}$	$E^{(1)}_{red}$	$E^{(2)}_{red}$	$E^{(3)}_{red}$
2a	0.01	−0.41	−1.36	−1.72
2b	0.02	−0.42	−1.35	−1.74
$Ce@C_{82}$[c]	0.08	−0.41	−1.41	−1.53

[a] Values are given in volts relative to a ferrocene/ferrocenium redox couple and were obtained from DPVs. [b] Conditions: working electrode and counter electrode, platinum wires; reference electrode, SCE; supporting electrolyte, 0.1 M $TBAPF_6$ in ODCB. CV: scan rate, 50 mV s^{-1}. DPV: pulse amplitude, 50 mV; scan rate, 20 mV s^{-1}. [c] Data from ref 18i.

The ESR signals due to the unpaired electron of the carbon cage in **2a** and **2b** were not detected, as in the case of $Ce@C_{82}$, because of broadening due to the remaining orbital angular momentum of the 4f electron on the Ce atom.[18i]

The redox potentials of **2a** and **2b** obtained from the DPVs are shown in Table 1. The first reduction potentials of **2a** and **2b** were almost unchanged from those of pristine $Ce@C_{82}$, indicating that the introduction of the Ad group has no important influence on the electron-accepting properties. The first oxidation potentials of **2a** and **2b** were cathodically shifted from that of $Ce@C_{82}$, suggesting an increase in the electron-donating properties. The CVs of both **2a** and **2b** exhibited three one-electron reduction and one oxidation reversible waves, as in the $Ce@C_{82}$

(26) Frisch, M. J.; et al. *Gaussian 03*, revision C. 01; Gaussian, Inc.: Wallingford, CT, 2004.
(27) Becke, A. D. *Phys. Rev. A* **1988**, *38*, 3098.
(28) Becke, A. D. *J. Chem. Phys.* **1993**, *98*, 5648.
(29) Lee, C.; Yang, W.; Parr, R. G. *Phys. Rev. B* **1988**, *37*, 785.
(30) Dolg, M.; Stoll, H.; Savin, A.; Preuss, H. *Theor. Chim. Acta* **1989**, *75*, 173.
(31) Binkley, J. S.; Pople, J. A.; Hehre, W. J. *J. Am. Chem. Soc.* **1980**, *102*, 939.

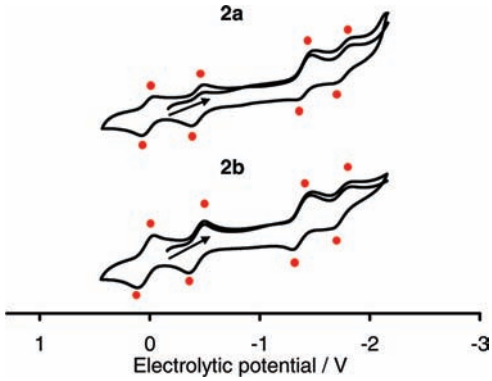

Figure 3. CVs of (top) **2a** and (bottom) **2b**.

case (Figure 3). It is also notable that the difference between the addition positions in **2a** and **2b** does not influence the electronic properties, which is in good agreement with the results of the absorption spectra.

The paramagnetic nature of the carbon cages of **2a** and **2b** does not allow direct NMR analysis, so their anions, [**2a**]$^-$ and [**2b**]$^-$, were prepared by the bulk electrolysis method. Both [**2a**]$^-$ and [**2b**]$^-$ showed clear bathochromic shifts in the absorption maxima relative to **2a** and **2b** (Figure S3 in the Supporting Information). It is very interesting to note that the ^{1}H NMR signals of [**2a**]$^-$ and [**2b**]$^-$ appeared in the extremely high field region between −2 and −15 ppm at room temperature (Figure 4), which is ascribed to the interplay between the f-electron spin on the Ce atom and the nuclear spins on the hydrogen atoms. This phenomenon was beneficial for the ^{1}H NMR observations because it enabled us to observe the signals of the methylene and methyne protons on the Ad group even if when proton signals of electrolytes or solvents overlapped them. Indeed, for [**3a**]$^-$ and [**3b**]$^-$, the proton signals of Ad groups were not observed because of the overlapping.

^{13}C enrichment of cage carbons enabled us to observe the ^{13}C NMR signals of [**2a**]$^-$ and [**2b**]$^-$ despite their low solubilities and the paramagnetic broadening of signals by the f-electron on the Ce atom. The ^{13}C NMR spectrum of [**2a**]$^-$ showed a total of 82 lines for the C_{82} cage, indicating that [**2a**]$^-$ has C_1 symmetry (Figure 5), while that of [**2b**]$^-$ showed 43 lines for the cage, indicating its C_s symmetry (Figure 6). The signals of the two sp^2 carbon atoms at the addition position of [**2a**]$^-$ were observed in the high-field region at 2 and −14 ppm at 293 K, providing evidence of the strong paramagnetic interaction between the two carbon atoms and the f electron on the Ce atom. On the other hand, the two signals of the sp^2 carbon atoms of [**2b**]$^-$ could not be detected because they were obscured by peaks due to impurities, such as the solvent and the electrolyte (as further discussed below). The signals of the C_{82} cage of [**2a**]$^-$ were distributed in the wide region from 65 to 210 ppm, except for those in the high-field region due to the two sp^2 carbon atoms at the addition position. In contrast, the distribution of the [**2b**]$^-$ dignals is considerably narrower (i.e., 100 to 177

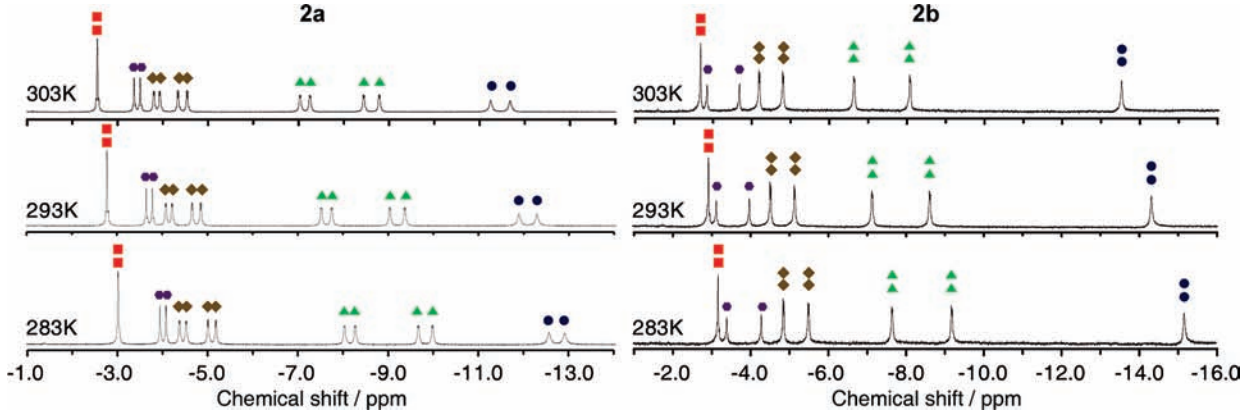

Figure 4. Temperature-dependent ^{1}H NMR spectra of (left) [**2a**]$^-$ and (right) [**2b**]$^-$ in 1:3 (v/v) acetone-d_6/CS_2. Colored symbols correspond to those in Figures 11 and 12.

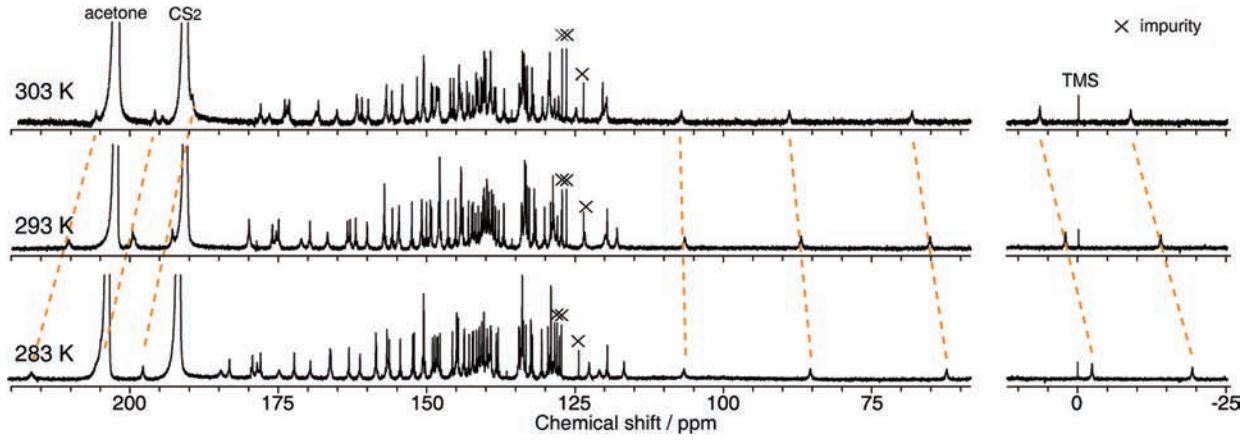

Figure 5. Temperature-dependent ^{13}C NMR spectra of [**2a**]$^-$ in 1:3 (v/v) acetone-d_6/CS_2. The signals due to the sp^2 carbon atoms on the cage are shown.

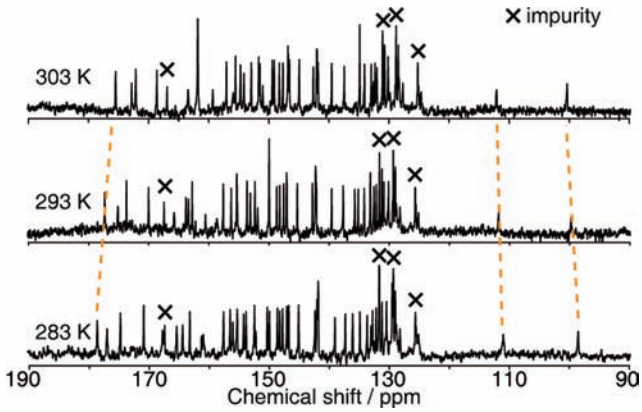

Figure 6. Temperature-dependent ^{13}C NMR spectra of $[\mathbf{2b}]^-$ in 1:3 (v/v) acetone-d_6/CS_2. The signals due to the sp^2 carbon atoms on the cage are shown.

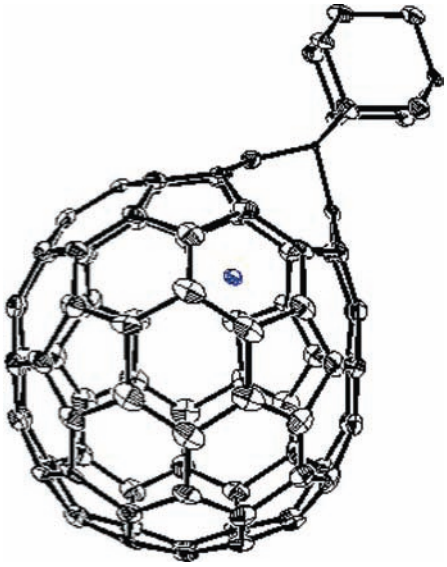

Figure 7. ORTEP drawing of $[\mathbf{2b}]^-$ at the 50% probability level. Hydrogen atoms on the Ad group, CS_2, and the countercation have been omitted for clarity.

ppm). These different paramagnetic shifts are ascribed to the fact that $[\mathbf{2a}]^-$ and $[\mathbf{2b}]^-$ have different addition positions.

The ORTEP drawing clearly shows that $[\mathbf{2b}]^-$ is a 6,6-adduct with an open structure having C_s symmetry (Figure 7). This is in good agreement with the NMR spectroscopy results and the optimized structure calculated at the B3LYP/3-21G∼SDD level (Figure 8b). This addition site is exactly the same as that we proposed for **3b** in the previous report,[23b] supporting the similarity in the selectivities of carbene addition to La@C_{82} and Ce@C_{82}.

Table 2 (with atom numbering given in Figure 9) shows values of the Mulliken charge density and the π-orbital axis vector (POAV) angle ($\theta_{\Delta\pi} - 90°$) in Ce@C_{82}.[32] The C2 atom has the most positive charge and the largest POAV angle. This suggests that the C2 atom is selectively attacked by **1** as an electrophile. Therefore, it is most feasible that the addition of the Ad carbene onto Ce@C_{82} takes place at the C1−C2 bond (bond A) or the C2−C3 bond (bond B). Indeed, the addition takes place between C2 and C3, as indicated by the X-ray crystal structure of $[\mathbf{2b}]^-$. On the other hand, carbene addition at bond

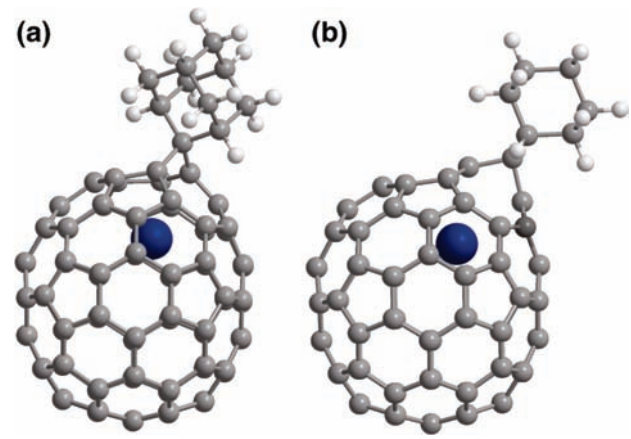

Figure 8. Optimized structures of (a) **2a** and (b) **2b** obtained using DFT calculations at the B3LYP/3-21G∼SDD level. Structure (b) was found to be 2.72 kcal/mol more stable than structure (a).

Table 2. Charge Densities (ρ, in e/Å^3) and POAV Angles (deg) in Ce@C_{82}

atom	ρ	POAV	atom	ρ	POAV	atom	ρ	POAV
C1	−0.152	11.74	C9	0.004	9.83	C17	−0.029	8.25
C2	−0.206	11.54	C10	−0.002	10.68	C18	0.006	11.01
C3	−0.136	8.41	C11	−0.009	10.62	C19	−0.004	10.90
C4	−0.102	9.39	C12	0.001	10.98	C20	−0.023	8.39
C5	−0.012	8.61	C13	−0.034	7.75	C21	0.004	10.49
C6	−0.011	10.32	C14	0.004	11.13	C22	−0.004	10.72
C7	−0.072	8.88	C15	−0.010	10.68	C23	0.008	10.72
C8	−0.040	8.78	C16	−0.021	7.44	C24	−0.023	8.31

A leads to the major isomer **2a**, on the basis of the fact that the C1 atom has more positive charge and a larger POAV angle than C3. The DFT calculations showed that **2a** and **2b** are the most stable and that **2b** is 2.72 kcal/mol more stable than **2a**. The thermal isomerization of **2a** to **2b** was also examined. After **2a** was heated at 250 °C for 12 h, a mixture of **2a** (20%) and **2b** (80%) was obtained (Figure S4 in the Supporting Information). Decomposition of the adducts to pristine Ce@C_{82} was not observed. This shows the high thermal stabilities of **2a** and **2b**.

The ^1H and ^{13}C NMR chemical shifts (δ) of $[\mathbf{2a}]^-$ and $[\mathbf{2b}]^-$ are temperature-dependent as a result of the buried f-electron spin remaining on the $Ce^{3+}(4f^15d^06s^0)$ atom. The chemical shift of a paramagnetic molecule in solution is generally expressed as a sum of three contributions, namely, the diamagnetic (δ_{dia}), Fermi contact (δ_{fc}), and pseudocontact (δ_{pc}) shifts, where the

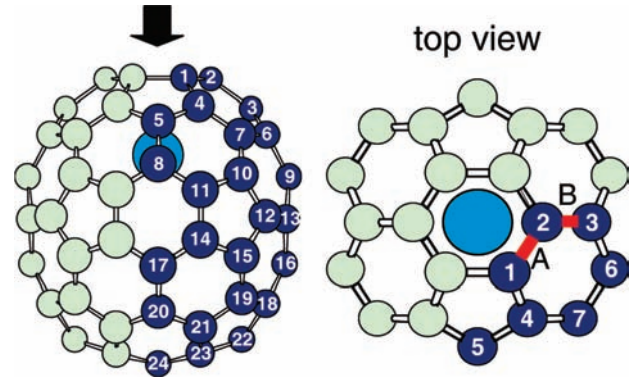

Figure 9. Schematic drawings and atom numbering of Ce@C_{82}.

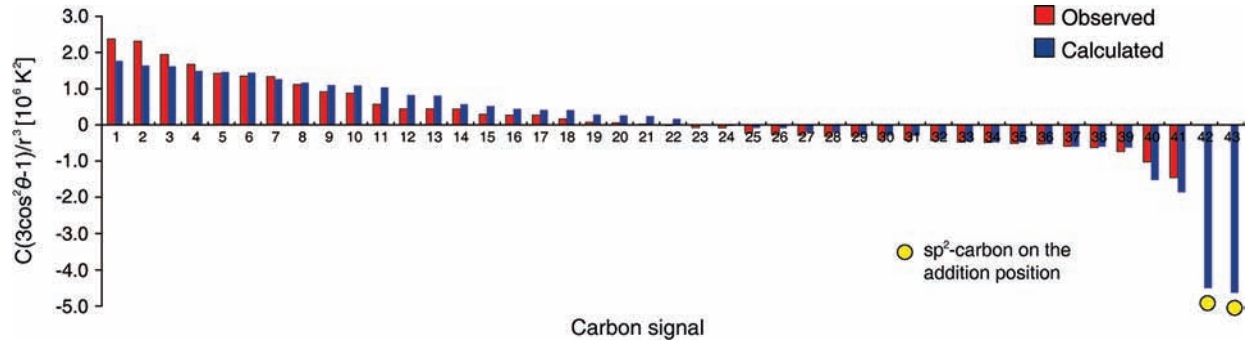

Figure 10. Observed (red) and calculated (blue) values of the proportionality constant between δ_{pc} and T^{-2} for the signals in the ^{13}C NMR spectrum of $[\mathbf{2b}]^-$. The values are arranged in decreasing order. The two signals due to the sp^2 carbon atoms at the addition position of the cage (numbered 42 and 43) were not clearly observed because they were obscured by the signals from the electrolyte and acetone solvent.

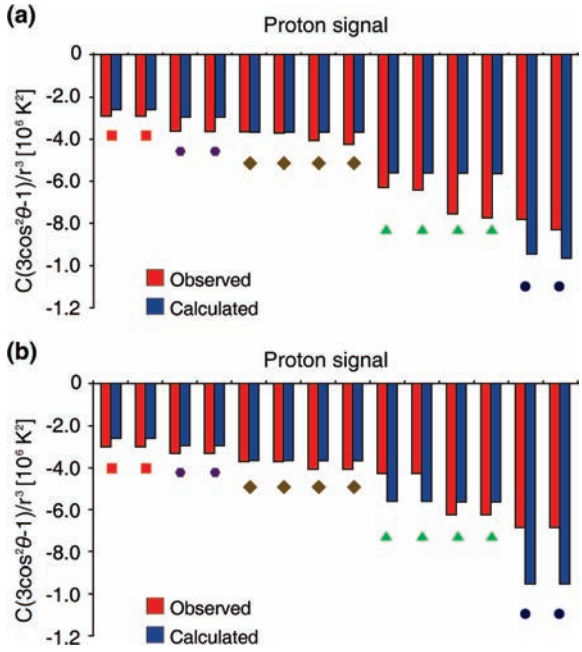

Figure 11. Observed (red) and calculated (blue) values of the proportionality constant between δ_{pc} and T^{-2} for the ^1H NMR signals of (a) $[\mathbf{2a}]^-$ and (b) $[\mathbf{2b}]^-$. The observed proton signals are listed in order of chemical shifts at 303 K, and the calculated values are listed in descending order. The colored symbols in (a) and (b) correspond to those in Figures 4 and 12, respectively.

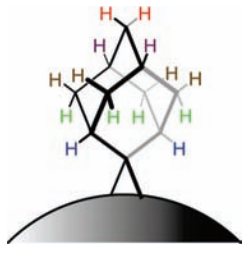

Figure 12. Schematic drawing of the Ad group. Atom colors correspond to the colored symbols in Figures 4 and 11.

paramagnetic shifts δ_{fc} and δ_{pc} are proportional to T^{-1} and T^{-2}, respectively (eq 1).[33]

$$\delta = \delta_{dia} + \delta_{fc} + \delta_{pc} \quad (1)$$

The δ_{dia} values in eq 1 were obtained from the ^{13}C NMR chemical shifts of $[\mathbf{3a}]^-$ and $[\mathbf{3b}]^-$.[23] As examples of paramagnetic NMR spectral analysis of EMFs, analyses for Ce@C_{82} and Ce_2@C_{80}Ad have been reported recently.[20,34] δ_{pc} makes a much larger contribution than δ_{fc} to the chemical shift for both $[\mathbf{2a}]^-$ and $[\mathbf{2b}]^-$, as shown by the analysis of the values at $T^{-1} = 0$ and $T^{-2} = 0$ obtained by extrapolation in the line-fitting plots of δ with respect to T^{-1} and T^{-2}, respectively (Figure S5 in the Supporting Information). The contributions of δ_{fc} are implied in the temperature dependence of the ^1H NMR spectra of $[\mathbf{2a}]^-$ and $[\mathbf{2b}]^-$ (Figure S6 in the Supporting Information). The underestimated values of δ_{pc} at $T^{-2} = 0$ obtained from δ_{dia} by extrapolation in the line-fitting plot with respect to T^{-2} (below $\delta = 0.8$ ppm in the results for both $[\mathbf{2a}]^-$ and $[\mathbf{2b}]^-$) are supplemented by δ_{fc}, giving rise to positive chemical shifts at $T^{-1} = 0$.

The δ_{pc} shifts of $[\mathbf{2a}]^-$ and $[\mathbf{2b}]^-$ can be briefly written as

$$\delta_{pc} = \frac{C(3\cos^2\theta - 1)}{r^3T^2} \quad (2)$$

where r is the distance between the Ce atom and the cage carbon, θ is the angle between the **r** vector and the vertical axis on which the Ce atom and the spiro carbon on the Ad group are located, and C is a common constant with a negative value for all cage carbons ($C = -6.827 \times 10^{-7}$ Å^3 K^2). Figure 10 shows observed and calculated values of the proportionality constant between δ_{pc} and T^{-2}, namely, $C(3\cos^2\theta - 1)/r^3$, for each observed carbon signal of $[\mathbf{2b}]^-$. The calculated δ_{pc} shifts were obtained using the r values from the DFT-optimized structures of $[\mathbf{2a}]^-$ and $[\mathbf{2b}]^-$. The calculated δ_{pc} values for $[\mathbf{2b}]^-$ are in very good agreement with the observed ones. This result provides the prediction for the ^{13}C NMR chemical shifts of the two missing signals for the sp^2 carbon atoms at the addition position of $[\mathbf{2b}]^-$. According to the calculated δ_{dia} and δ_{pc} values, these signals are expected to appear at ~30 and ~41 ppm at 293 K, where the large peaks due to the solvent and the electrolyte can obscure them. For $[\mathbf{2a}]^-$, although it was not possible to analyze all of the signals because of the complexity of the spectral pattern, the observed and calculated values showed a tendency for the δ_{pc} shifts similar to that for $[\mathbf{2b}]^-$ (Figure S7 in the Supporting Information). These results indicate that eq 2 is applicable to the analysis of the paramagnetic shifts in Ce@C_{82} derivatives.

In addition, the ^1H NMR spectra could be assigned on the basis of the paramagnetic shifts by comparing the calculated and observed values of $C(3\cos^2\theta - 1)/r^3$ for each proton of $[\mathbf{2b}]^-$ (Figure 11b). These values were found to be the largest for the protons in the bottom part of the Ad group (colored

blue in Figure 12) and the smallest for those in the top part of the Ad group (colored red in Figure 12). Because each of these two positions has two equivalent protons, the singlet signal at $\delta = -14.31$ ppm is surely attributable to the protons in the bottom part of the Ad group and the signal at -2.91 ppm to those in the top part. The signals at -3.11 and -3.97 ppm are due to the two inequivalent protons in the upper part on the mirror plane (colored purple in Figure 12) on the basis of their half-signal intensities. Of the remaining eight protons, the four positioned farther from the Ce atom (colored brown in Figure 12) give rise to the peaks from -4 to -5 ppm on the basis of their smaller degree of upfield shifting, and the four nearer to the Ce atom (colored green in Figure 12) produce the signals at -7 to -9 ppm on the basis of their larger upfield shifting. In a similar way, through the use of the values in Figure 11a, the proton signals of [**2a**]$^-$ can be roughly assigned as shown by the colored symbols in Figure 4 (which correspond to the color code in Figure 12), even though [**2a**]$^-$ has C_1 symmetry and all of the hydrogen atoms are nonequivalent.

Conclusion

Two isomers of Ce@C_{82}Ad (**2a** and **2b**) were synthesized in high yields by a carbene addition reaction. **2a** and **2b** were fully characterized by spectroscopic methods. Interestingly, the chemical reactivity of Ce@C_{82} is similar to that of La@C_{82}, although the encapsulated metals are different. Paramagnetic shifts in ^{1}H and ^{13}C NMR spectra were observed for [**2a**]$^-$ and [**2b**]$^-$, reflecting the anisotropic behavior of the f-electron spin on the Ce atom. The observations of paramagnetic shifts help reveal the magnetic properties of metal-encapsulating carbon clusters, as demonstrated by structural and substituent effects on Ce@C_{82} derivatives.

Acknowledgment. This work was supported in part by a Grant-in-Aid for Scientific Research on Innovative Areas (20108001, "π-Space"), a Grant-in-Aid for Scientific Research (A) (20245006), the 21st Century COE Program, the Next Generation Super Computing Project (Nanoscience Project), the Nanotechnology Support Project, Grants-in Aid for Scientific Research on Priority Areas (20036008, 20038007) from the Ministry of Education, Culture, Sports, Science, and Technology of Japan, and a grant from the Kurata Memorial Hitachi Science and Technology Foundation. M.Y. and H.N. thank the Japan Society for the Promotion of Science (JSPS) for Research Fellowships for Young Scientists.

Supporting Information Available: Crystallographic data for [**2b**]$^-$ (CIF); complete refs 5l, 23a, and 26; spectral data for **2a**, **2b**, and their anions; and Cartesian coordinates for **2a** and **2b**. This material is available free of charge via the Internet at http://pubs.acs.org.

JA902106A

(32) Haddon, R. C. *Science* **1993**, *261*, 1545.
(33) Bleaney, B. *J. Magn. Reson.* **1972**, *8*, 91.
(34) Yamada, M.; Someya, C.; Wakahara, T.; Tsuchiya, T.; Maeda, Y.; Akasaka, T.; Yoza, K.; Horn, E.; Liu, M. T. H.; Mizorogi, N.; Nagase, S. *J. Am. Chem. Soc.* **2008**, *130*, 1171.